Synchronized Signal Control Model for Maximizing Progression along an Arterial

Liang-Tay Lin[1]; Li-Wei (Chris) Tung, A.M.ASCE[2]; and Hsin-Chuan Ku[3]

Abstract: For the most part, optimal signal timing is the most effective and economical method for mitigating traffic congestion in urban areas. In this study, a new mixed integer nonlinear programming model is proposed to develop an optimal arterial-based progression algorithm. The proposed algorithm is designed to optimize the bandwidths for contiguous signals along a signalized arterial. The traffic conditions for examining the proposed algorithm are extracted from moderate to high saturated traffic conditions. The main objective of the proposed algorithm is to allow traffic to traverse through the maximum number of downstream intersections without a stop. According to measures of effectiveness (MOE_s) acquired by TSIS-CORSIM 6, the signal timing generated by the proposed model yields lower stops (%) when compared with the signal timing optimized and generated by Synchro. In addition, the proposed model yields lower network-wide average delays (sec/veh) and higher average travel speeds (km/h) under moderate to high saturated traffic conditions. The performance and applicability of the proposed model have been validated.

DOI: 10.1061/(ASCE)TE.1943-5436.0000123

CE Database subject headings: Traffic signals; Time factors; Economic factors; Traffic congestion; Urban areas.

Author keywords: Bandwidth; Traffic signal timing; Progression bandwidth.

Introduction

Various models are used to mitigate traffic congestion in urban areas. The objectives of these models are mainly to minimize vehicle delay and maximize intersection performance. Therefore, in this paper, a new arterial-based progression algorithm, mixed integer nonlinear programming (MINLP), designed to optimize the progression bandwidths for the contiguous signals along a signalized arterial, is introduced. The proposed algorithm is expected to minimize the number of stops, minimize network-wide average delay, and maximize average travel speed. It also provides better progression schemes to roadway users. The traffic conditions are extracted from moderate to high saturated traffic conditions to validate the feasibility of the proposed model.

Background

In general, two conventional signal timing approaches, delay minimization and progression bandwidth maximization, are used to coordinate traffic signals and optimize traffic signal timing. Delay-oriented signal timing may require minimizations in delay, stop, and queue length. Bandwidth-oriented signal timing requires optimization of four signal timing parameters (e.g., cycle length, green split, offset, and phase sequence). Roess et al. (2004) defined the bandwidth as "The time between the first and the last vehicle that pass through the entire arterial system without stopping." As bandwidth-oriented signal timing is meant to obtain the maximum bandwidths in both directions, Little (1966) proposed a theory of maximum progression bandwidth to maximize two-way arterial progression using a mixed integer linear program. Pillai et al. (1998) presented a numerically stable heuristic for the maximum bandwidth signal setting problem. It is based on restricted search of the integer variables in the solution space. Gartner et al. (1991), Stamatiadis and Gartner (1996), and Gartner and Stamatiadis (2002) used the maximum progression bandwidth and established a variable bandwidth (or multiband) for objective function and green time revision to adapt to all kinds of traffic conditions. Gartner and Stamatiadis (2004), then, proposed several procedures for traffic signal optimization (both uniform- and variable-bandwidth optimization) in grid networks. The programs use advanced mathematical programming models which are computationally demanding when applied to large-scale networks.

Tsay and Lin (1988) divided the time between the beginning of green time and the beginning of bandwidth into two parts: queue clearance time (Q_i) and incoming flow clearance time (H_i). Their model provided for an exclusive time for vehicles queuing on a major-street approach to completely discharge and leave the intersection. Any vehicle in the segment is allowed to traverse through the entire signalized arterial with a maximum of one stop. However, with an increased number of signals on an arterial and/or increased queue length at an approach, there may be difficulty in optimizing and synchronizing the bandwidths in both directions. Tian and Urbanik (2007) proposed a new method of dividing a major system into several subsystems to solve such problems. By optimizing subsystems' bandwidths and adjusting offsets between subsystems, CORSIM simulation results indicate

[1]Associate Professor, Dept. of Transportation Technology and Management, Feng Chia Univ., Taichung 407, Taiwan (corresponding author). E-mail: ltlin@fcu.edu.tw

[2]Project Engineer, Riedesel Engineering, Twin Falls, Idaho 83301. E-mail: LTung@Riedeseleng.com

[3]Graduate Research Assistant, Dept. of Transportation Technology and Management, Feng Chia Univ., Taichung 407, Taiwan. E-mail: hsinchuanku@gmail.com

Note. This manuscript was submitted on March 6, 2009; approved on October 12, 2009; published online on October 14, 2009. Discussion period open until January 1, 2011; separate discussions must be submitted for individual papers. This paper is part of the ***Journal of Transportation Engineering***, Vol. 136, No. 8, August 1, 2010. ©ASCE, ISSN 0733-947X/2010/8-727–735/$25.00.

J. Transp. Eng. 2010.136:727-735.

accurate and effective measurement of bandwidth maximization. Then, Tian et al. (2008) proposed a computer program to randomly generate multiple signal system scenarios randomly and to provide maximum bandwidth solutions. The randomly generated signal system scenarios represent various signal systems likely to be seen in the real world.

In general, bandwidth-oriented signal planning is preferred as it provides more progression opportunities for traffic on major streets. Bandwidth-oriented signal timing mainly considers major-street approaches, possibly producing higher delays on minor-street approaches. Yang (2001) applied both delay- and bandwidth-oriented approaches to nine intersections and found that the bandwidth-oriented signal timing approach generally outperformed the delay-oriented signal timing approach.

Although these two conventional approaches have individual strengths and shortcomings, bandwidth-oriented signal timing is preferred by traffic engineers and drivers because it meets drivers' expectations for traversing through the arterial with fewer stops. As a result, traffic engineers usually judge the performance of a signal coordination system by the efficiency of progression bandwidths. Additionally, if signalized arterials do not possess adequate progression bandwidths, the function of signal timing is limited. While taking both delay-oriented and bandwidth-oriented planning into consideration, the bandwidth-oriented signal timing is used in this study since the signal timing is easily optimized and judged by engineers through time-space diagrams.

This paper enhances the maximum progression bandwidth algorithm proposed by Tsay and Lin (1988). Our proposed algorithm will overcome the shortcoming of that model, namely, the inability to provide contiguous progression bandwidths throughout the whole arterial, and allow traffic streaming through the maximum number of downstream intersections without a stop. The revised algorithm is also designed to optimize the signal timing and to provide a better signal coordination scheme for urban areas. While the model is prepared, a data processing and validation step is conducted to examine the performance. The average travel speed (km/h), network-wide average delay (sec/veh) and stops (%) are the measures of effectiveness (MOE_s) used to evaluate the final performance. Five different cases are selected as experimental scenarios.

Methodology

As the number of signals on an arterial and/or queue length increases, it becomes increasingly difficult to achieve realistic progression bands in both traffic directions. In order to overcome this problem, the maximum progression algorithm proposed by Tsay and Lin (1988) is modified in terms of objective function, constraints, and calculations. By applying the new proposed maximum progression model to an arterial, the model yields more flexibility in solving and enhancing the efficiency of progression bandwidths. It is especially suitable for addressing user perspective which is only concerned with how many intersections can be traversed without stopping under moderate to high saturated traffic conditions. All experiments are conducted at fixed-time signalized intersections, and the following six assumptions are made prior to applying the model:

1. The arrival sequence is in a uniform pattern;
2. Each section can have different average travel speeds as compared to the other sections;
3. No platoon dispersion;
4. No midblock flow;

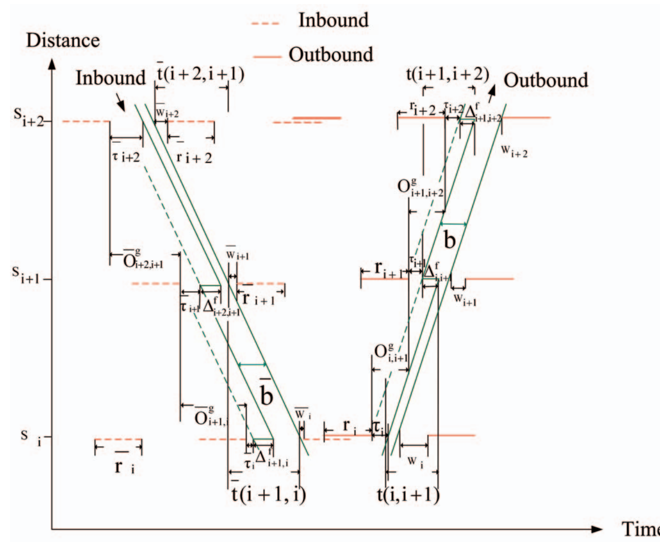

Fig. 1. (Color) Time-space diagram of maximum progression bands

5. The "First in, First out (FIFO)" discipline is used to discharge the platoon on each lane; and
6. Once vehicles enter a study section, no lane changing and/or overtaking is allowed.

The traffic signals on an arterial are denoted as $S_1, S_2, \ldots, S_i$. Fig. 1 shows the time-space diagram of the maximum progression bands. The definitions of variables are as follows:

- S_i=ith signal ($i=1,2\ldots n$);
- $r_i(\bar{r}_i)$=outbound (inbound) red time at S_i;
- $g_i(\bar{g}_i)$=outbound (inbound) green time at S_i;
- $\tau_i(\bar{\tau}_i)$=outbound (inbound) queue clearance time ratio at S_i;
- $b(\bar{b}_i)$=outbound (inbound) bandwidth between Si and S_{i+1} signal;
- $W_i(\bar{W}_i)$= time between the trailing edge of the outbound (inbound) green band and the beginning of the following red interval at Si;
- $\Delta^f_{i,i+1}(\Delta^f_{i+1,i})$=the distance between the leading bands $S_i(S_{i+1})$ and $S_{i+1}(S_i)$;
- $\Delta^e_{i,i+1}(\Delta^e_{i+1,i})$=the distance between the trailing bands $S_i(S_{i+1})$ and $S_{i+1}(S_i)$;
- $t_{(i,i+1)}(\bar{t}_{(i,i+1)})$=travel time from S_i to S_{i+1} in outbound (inbound) direction;
- $t_{(i+1,i+2)}(\bar{t}_{(i+1,i+2)})$=travel time from S_{i+1} to S_{i+2} in outbound (inbound) direction;
- $O^g_{i,i+1}(\bar{O}^g_{i,i+1})$=outbound (inbound) green time (g) offset (O) between S_i and S_{i+}; and
- $O^g_{i+1,i+2}(\bar{O}^g_{i+1,i+2})$=outbound (inbound) green time (g) offset (O) between S_{i+1} and S_{i+2}.

In Fig. 1, the model delivers a long bandwidth in both inbound and outbound directions and provides an opportunity for traffic to traverse S_i to S_{i+2} without stopping.

The proposed model can be applied to both major-street approaches and minor-street approaches. However, major-street approaches have higher traffic demands than minor-street approaches, and may have higher probabilities of maximizing progression bandwidths. Thus, longer delays may be detected on minor-street approaches. Applying adequate adjustments in signal split can mitigate such delays. An overall proposed model is presented in the appendix.

J. Transp. Eng. 2010.136:727-735.

Objective Function

In the objective function, this paper introduces two criteria to the model: (1) the maximum number of intersections that vehicles can traverse through without stopping; and (2) the discipline of arrival sequence. The equation of the objective function is presented below

$$\sum_{i=1}^{n}[P_i+\overline{P_i}+k\times\max(Q_{i,m}^{\text{inbound}},Q_{i,m}^{\text{outbound}})] \quad i=1\ldots n \quad (1a)$$

where $P_i(\overline{P_i})$=maximum number of intersections (on the major street) that vehicles at the ith intersection can traverse through in the outbound (inbound) direction without stopping; k=volume ratio between major- and minor-street approaches; and $Q_{i,m}^{\text{inbound}}(Q_{i,m}^{\text{outbound}})$=fraction of queued vehicles (Q) passing the ith intersection from the inbound (outbound) minor-street approach (m).

The first part of the objective function, $\Sigma_{i=1}^{n}[P_i+\overline{P_i}]$, represents the maximum number of intersections that vehicles on the major street can traverse through without stopping. The second part of the objective function, $\Sigma_{i=1}^{n}[k\times\max(Q_{i,m}^{\text{inbound}},Q_{i,m}^{\text{outbound}})]$, represents whether or not all vehicles queuing on the inbound and/or outbound minor-street approaches can traverse through the ith intersection in one green interval. It also prevents the traffic controller from allocating the majority of green time to major-street approaches. The parameter k represents the volume ratio between the major- and minor-street approaches. In this study, the initial green splits are generated by the model of Webster and Cobbe (1966). The function of the parameter k is used to confirm that the green splits generated by Webster's formulation are adequately allocated to both major-and minor-street approaches, and can avoid producing longer delays on minor-street approaches. If splits do not satisfy the actual traffic demands and/or the minimum green times determined by the number of pedestrians, further modifications in green splits should be made. As an example of the volume ratio (k) calculation, if at a fixed-time signalized intersection, the demand is 360 vehicle-per-hour (VPH) on a minor-street approach and 1800 VPH on a major-street approach, the value of the parameter k is equivalent to 0.2 (=360/1800).

Constraints

In this section, all constraints used in this model are introduced. Each constraint is defined in the following subsections.

Composition of Green Time

As the number of signals on an arterial increase and/or when the queue clearance time at any traffic signal uses most of the green split, it becomes increasingly difficult to achieve realistic progression bands. In order to overcome this problem, different stages of flow are assigned per green interval. A green interval is assigned to combine the queue clearance time (τ), the bandwidth of two adjacent intersections (b), and the time between the trailing edge of the outbound (inbound) green band and the beginning of the following red interval (W), as shown in Fig. 1. All three variables (τ, b, and W) and other time related variables (e.g., r, g, $\Delta_{i-1,i}^{e}$, $\Delta_{i-1,i}^{f}$) are presented as fractions while applying to all calculations in the proposed model. Three variables and other time related variables are the numerators, and the cycle length is the denominator. The cycle length for all intersections along a study arterial is identical as will be discussed next. The formula, Eq. (1b), is as follows:

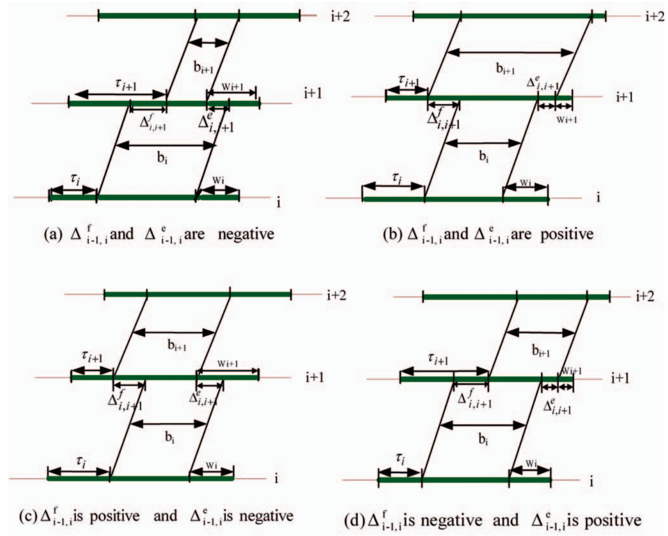

Fig. 2. (Color) Intersection relationships

$$g_i=\tau_i+b_i+W_i \quad (1b)$$

where g_i=green time at the ith intersection; $\tau_i(\bar{\tau}_i)$=outbound (inbound) queue clearance time at the ith intersection; $b_i(\bar{b}_i)$ =outbound (inbound) bandwidth between the $(i-1)$th and the ith intersections; and $W_i(\bar{W}_i)$=time between the trailing edge of the outbound (inbound) green band and the beginning of the following red interval at the ith intersection.

Intersection Relationship

The flow stage in a green interval at an intersection varies depending on the adjacent intersection. Eq. (1c) indicates that the difference between two successive green bands is associated with the variations in the leading edge ($\Delta_{i-1,i}^{f}$) and the trailing edge ($\Delta_{i-1,i}^{e}$), as shown in Fig. 1

$$b_i=\Delta_{i-1,i}^{f}+b_{i-1}+\Delta_{i-1,i}^{e} \quad (1c)$$

where $\Delta_{i-1,i}^{f}$=time difference between the leading edges (f) of the green bands at the ith and $(i+1)$th intersections; and $\Delta_{i-1,i}^{e}$=time difference between the trailing edges (e) of the green bands at the ith and $(i+1)$th intersections.

The two delta pairs, two leading edges ($\Delta_{i-1,i}^{f}$) and two trailing edges ($\Delta_{i-1,i}^{e}$) at intersections S_{i-1} and S_i can be expressed as a range and are shown in Eqs. (1d) and (1e)

$$-g_i+\tau_i\leq\Delta_{i-1,i}^{f}\leq g_i-\tau_i \quad (1d)$$

$$-g_i+\tau_i\leq\Delta_{i-1,i}^{e}\leq g_i-\tau_i \quad (1e)$$

In Eqs. (1c) to (1e), the two variables $\Delta_{i-1,i}^{f}$ and $\Delta_{i-1,i}^{e}$ range between 1 and -1. By using these two variables in association with the originally designed green bandwidths, the results reflect the different traffic flow conditions. Four types of intersection relationships between two adjacent intersections are discussed in this study and are illustrated in Figs. 2(a–d). In Fig. 2(a), the leading edge of the green band at intersection i occurs earlier than the one at intersection $i+1$. The trailing edge of the green band at inter-

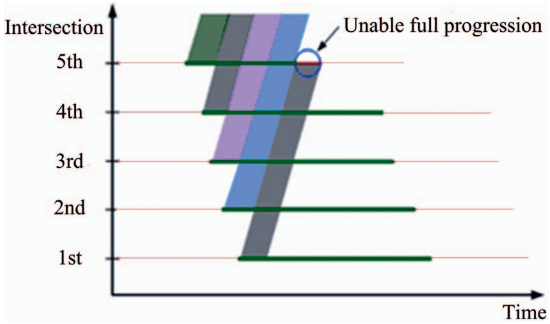

Fig. 3. (Color) Sequence of green time at each intersection

section $i+1$ occurs earlier than the one at intersection i. In addition, intersection $i+1$ needs longer queue clearance time (τ_{i+1}) than intersection i (τ_i). The available bandwidth (b_{i+1}) at intersection $i+1$ is apparently insufficient to progress the traffic coming from intersection i. Therefore, the $\Delta^f_{i-1,i}$ and $\Delta^e_{i-1,i}$ values in Fig. 2(a) are negative. In Fig. 2(b), the leading edge of the green band at intersection $i+1$ occurs earlier than the one at intersection i. The trailing edge of the bandwidth at intersection i also occurs earlier than the one at intersection $i+1$. In addition, intersection i needs longer queue clearance time (τ_i) than intersection $i+1$. The available bandwidth (b_{i+1}) at intersection $i+1$ is apparently sufficient to progress the traffic coming from intersection i. Therefore, the $\Delta^f_{i-1,i}$ and $\Delta^e_{i-1,i}$ values in Fig. 2(b) are positive. The values of $\Delta^f_{i-1,i}$ and $\Delta^e_{i-1,i}$ in Figs. 2(c and d) can be determined using the same concepts.

Common Cycle

Each coordinated signalized intersection should be associated with an identical cycle length. As mentioned previously, all three variables (τ, b, and W), red time (r), and green time (g) are presented as fractions

$$\tau_i + b_i + W_i + r_i = 1 \qquad (1f)$$

$$\bar{\tau}_i + \bar{b}_i + \bar{W}_i + \bar{r}_i = 1 \qquad (1g)$$

Stage of Green Time at Each Intersection

At the beginning of each green time period, each intersection should discharge its existing queued vehicles, and then start processing the traffic coming from upstream intersections until the green time period has ended. The sequence of green time at each intersection is shown in Fig. 3.

In Fig. 3, the progression area at each individual intersection is defined as the green time minus the queue clearance time. The progression area can be divided into two types, type 1 and type 2. Type 1 is defined as "progression band starting from its original intersection that can completely allow traffic traversing through the last intersection on an arterial without impedance." The light blue belt in Fig. 3, for example, represents the progression band starting from the second intersection which can completely allow traffic traversing through the last intersection (the fifth intersection) on a signalized arterial. In contrast, if a vehicle cannot reach the last intersection in a single progression opportunity, this is type 2. The gray belt in Fig. 3 represents type 2, where the progression band starts from the first intersection and ends at the fourth intersection. Traffic cannot completely traverse through the fifth intersection. Four cases have been selected and are illustrated in Fig. 4.

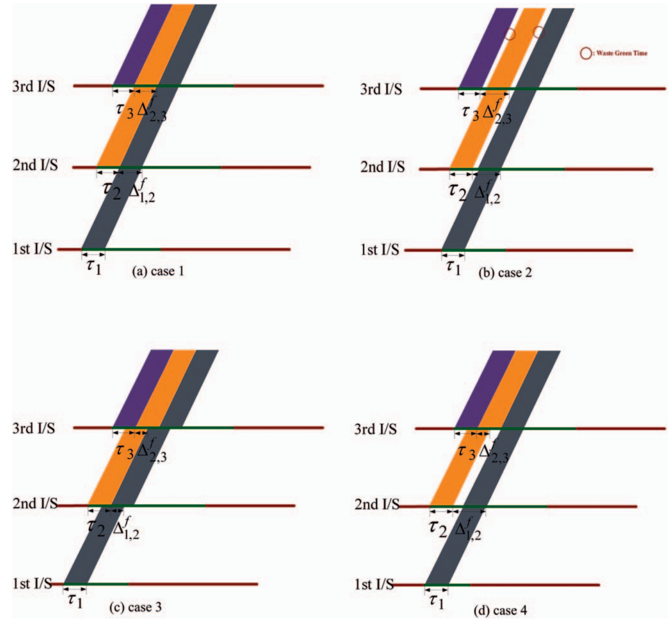

Fig. 4. (Color) Cases for the stages of green time at each intersection

Case 1: Upstream Bands Projected to Arrive after Downstream Queue Discharges

Fig. 4(a) shows that after discharging the queued vehicles at the third intersection, the progression bands coming from the upstream intersections (e.g., the first and second intersections) arrive at the third intersection immediately without wasting any green time at the third intersection. This situation can be implied as $\Delta^f_{2,3}=\tau_2$. In addition, the number (j) used to represent the last downstream intersection that traffic can traverse through is greater than the number (i) used to represent the beginning (or upstream) intersection. Then, if $\Delta^f_{i,j}=\tau_i$ and $j>i$, the result will belong to Case 1.

Case 2: Upstream Bands Projected to Not Arrive after Downstream Queue Discharges

Fig. 4(b) shows that after discharging the existing queued vehicles at the third intersection, the progression bands coming from the upstream intersections (e.g., the first and second intersections) do not arrive at the third intersection immediately and the green time is wasted. The gaps (red circles) between the first and second intersections and the second and third intersections represent the wasted green time. This situation can be implied as $\Delta^f_{2,3}>\tau_2$ and $\Delta^f_{1,2}>\tau_1$, respectively. If $\Delta^f_{i,j}>\tau_i$ and $j>i$, the result will belong to Case 2.

Case 3: Upstream Bands Projected to Arrive before Queue Discharges

Case 3 is defined as the situation in which queuing vehicles at the third intersection cannot be completely discharged before the upstream bands (e.g., the first and second intersections) arrive. This situation can be implied as $\Delta^{f}_{2,3} < \tau_2$. If $\Delta^{f}_{i,j} < \tau_i$ and $j > i$, the result will belong to Case 3.

Case 4: Combination of Case 1, Case 2, and Case 3

Case 4 combines the situations of Case 1, Case 2, and Case 3. As described in Cases 1–3, if $\Delta^{f}_{i+1,j+1} < \tau_{i+1}$, $j+1 > i+1$, and $\Delta^{f}_{i,j} > \tau_i$, $j > i$, the result will belong to Case 4.

According to the previous discussions, the final equation for different arrival types is given as Eq. (1h). All variables (i.e. d_i and e_{n-1}) are presented as fractions, and the denominator is the common cycle length.

$$\sum_{i=1}^{n-1}\left[\left(\prod_{j=i}^{n-1}\prod_{k\geq j}^{n-1} P_{jk}\right)\times d_i\right] + e_{n-1} = g_{n-1} \qquad (1h)$$

where g_{n-1}=green time at the $(n-1)$th intersection; d_i=time difference between the end of queue discharge and the arrival of upstream bands at the ith intersection (d_i, $i=1$ to $n-1$). For Cases 1, 3, and 4, queue clearance time (τ_i) is the value of d_i; for Case 2 $\Delta^{f}_{i,i+1}$ is the value of d_i; and e_{n-1}=remaining green time at the $(n-1)$th intersection on an arterial after all vehicles coming from upstream intersections are discharged. If there is no remaining green time, $e_{n-1}=0$.

In Eq. (1h), the parameter d_i can be determined by observing the difference between the end of queue discharge and the arrival of downstream progression bands from a contiguous signalized arterial. Under real-world traffic conditions, there are many situations that will prevent upstream vehicles from traversing through all coordinated intersections without stopping. However, by applying the concepts proposed in this study, the whole system can be classified and divided into certain subsystems according to their features to allow the traffic on an arterial to traverse through a maximum number of intersections in a single progression opportunity.

Average Queue Length

In order to avoid the situation of the queue length exceeding the length of a road section and detrimentally influencing the efficiency of queue discharge, this constraint needs to be added to our model. The constraint is defined as the average queue length on an approach in a signal cycle.

The queue length is categorized into two types

1. The average queue length on a major-street approach is the product of the average queue clearance time per cycle, average discharge rate per cycle, and average vehicle length. In this paper, the average vehicle length is assumed to be six meters.
2. The average queue length on a minor-street approach is the product of the red time (on minor-street approach), arrival rate, and average vehicle length.

Speed Limit

The speed limit constraint is used to determine the lower and upper speed limits when the model of maximum progression bandwidth is applied, as shown in Eqs. (1i) and (1j). If the speed limit is calculated to range between 45 km/h and 50 km/h, for example, the speed of 44km/h cannot reach the minimum limit for continuous maximum progression bandwidth

$$(D_i/f_i)Z \leq t_i \leq (D_i/m_i)Z \qquad (1i)$$

$$(\bar{D}_i/\bar{f}_i)Z \leq \bar{t}_i \leq (\bar{D}_i/\bar{m}_i)Z \qquad (1j)$$

where Z=signal frequency (the reciprocal of signal cycle, 1/C); D_i=distance (in meters) between S_i and S_{i+1}; and $m_i(\bar{m}_i)$, $f_i(\bar{f}_i)$ =lower and upper speed limits (km/h) in outbound (inbound) direction.

Through this constraint, the ranges of link travel time under different flow conditions can be determined to design adequate signal offsets on a contiguous signalized arterial, and to optimize maximum progression bandwidths.

Speed Change Limit

This constraint is used to ensure that speed changes between two adjacent segments fall into a reasonable range. For example, under an impeded (or free) flow condition in a contiguous signalized arterial, if a vehicle can maintain a speed of 40 km/h on Street A, when the vehicle enters Street B, the travel speed on Street B should be equivalent or close to 40 km/h, to avoid extremely large speed changes. The equations are as follows:

$$(D_i/h_i)Z \leq (D_i/D_{i+1})t_{i+1} - t_i \leq (D_i/n_i)Z \qquad (1k)$$

$$(\bar{D}_{i+1}/\bar{h}_{i+1})Z \leq (\bar{D}_{i+1}/\bar{D}_i)\bar{t}_i - \bar{t}_{i+1} \leq (\bar{D}_{i+1}/\bar{n}_{i+1})Z \qquad (1l)$$

where $(1/h_i, 1/n_i)$=lower $(1/h_i)$ and upper $(1/n_i)$ limits for the change in the reciprocal of speeds ($(\mathrm{m/sec})^{-1}$) between S_i and S_{i+1}. It can be represented as $1/h_i \leq (1/V_{i+1}) - (1/V_i) \leq 1/n_i$.

Minimum Green Time

This constraint is used to ensure that the minimum green time allocated on the minor-street approach is sufficient for pedestrians to safely cross the intersection

$$r_i - \Delta_i \geq \text{Min g}_i \qquad (1m)$$

where Min g_i=minimum green time on the minor-street approach at intersection i; and Δ=time between two centers (inbound and outbound) of red.

Calculations

The last part of the model is the calculations. The calculations include: (1) the calculation of queue clearance time and (2) the calculation of signal offset. The signal offset is also the ultimate production of the proposed model, and both are discussed in the following sections. All time related variables (e.g., O and t) are presented as fractions, and the denominator is the common cycle length.

Calculation of Queue Clearance Time

The queue clearance time is defined as the time to completely discharge the vehicles in queue at each approach. Using the queue clearance time, we can set up the optimal green time and also optimize the signal offset for two successive intersections. Then, minimum stops throughout the intersections during one progression bandwidth can be expected. It is essential to calculate the queue clearance time effectively. The queue clearance time is calculated using three variables: (1) major-street approach through movement; (2) minor-street approach left- and right-turn movements; and (3) signal offsets. Signal offsets in this calculation are

J. Transp. Eng. 2010.136:727-735.

Table 1. Possibilities of Queue Clearance Time Calculations

Situation		Queue clearance time (τ) at the $(i+1)$th intersection
$O^g_{i,i+1}>0$	$O^g_{i,i+1}\geq t_{i,i+1}$ and $O^r_{i,i+1}\geq t_{i,i+1}$	$[(O^g_{i,i+1}-t_{i,i+1})\times\lambda_a+(t_{i,i+1}+r_{i+1}-O^g_{i,i+1})\times\lambda_m]/S_a$
	$O^g_{i,i+1}\geq t_{i,i+1}$ and $O^r_{i,i+1}<t_{i,i+1}$	$[(O^g_{i,i+1}-O^r_{i,i+1})\times\lambda_a+r_i\times\lambda_m]/S_a$
	$O^g_{i,i+1}<t_{i,i+1}$ and $O^r_{i,i+1}\geq t_{i,i+1}$	$(r_{i+1}\times\lambda_m)/S_a$
	$O^g_{i,i+1}<t_{i,i+1}$ and $O^r_{i,i+1}<t_{i,i+1}$	$[(t_{i,i+1}-O^r_{i,i+1})\times\lambda_a+(r_{i+1}+O^r_{i,i+1}-t_{i,i+1})\times\lambda_m]/S_a$
$O^g_{i,i+1}<0$	$O^g_{i,i+1}\geq t_{i,i+1}$ and $O^r_{i,i+1}\geq t_{i,i+1}$	$[O^r_{i,i+1}\times\lambda_a+(r_i-O^g_{i,i+1})\times\lambda_m]/S_a$
	$O^g_{i,i+1}\geq t_{i,i+1}$ and $O^r_{i,i+1}<t_{i,i+1}$	$(r_{i+1}\times\lambda_a)/S_a$
	$O^g_{i,i+1}<t_{i,i+1}$ and $O^r_{i,i+1}\geq t_{i,i+1}$	$(r_{i+1}\times\lambda_a)/S_a$
	$O^g_{i,i+1}<t_{i,i+1}$ and $O^r_{i,i+1}<t_{i,i+1}$	$[(t_{i,i+1}-O^r_{i,i+1})\times\lambda_a+(r_{i+1}-t_{i,i+1}+O^r_{i,i+1})\times\lambda_m]/S_a$

categorized as: (1) positive signal offsets and (2) negative signal offsets. All possibilities of queue clearance time calculations are shown in Table 1. In Table 1, $O^g_{i,i+1}$ is the difference between the two green initiation times for the two successive intersections, intersections i and $i+1$. O in this variable is referred to as the signal offset. If $O^g_{i,i+1}$ is greater than zero, the offset (in green time) is positive. Similarly, $O^r_{i,i+1}$ is the difference between the two red initiation times for two successive intersections. The parameter $t_{i,i+1}$ represents the average travel time from intersections i to $i+1$. The parameter λ_a represents the traffic arrival rate (λ) on a major-street approach (a), and the parameter λ_m represents the traffic arrival rate on a minor-street approach (m). The parameter S_a represents the queue discharge rate on a major-street approach under saturated traffic conditions. In this study, traffic arrival type at all intersections is assumed to be uniform. The formulas shown in Table 1 can be applied to any two successive intersections.

Calculation of Offset

The signal offset is defined as the deviation of the beginning green time of a signal from a reference. By optimizing signal offset, traffic can smoothly traverse through the arterial with less impedance. The calculations of signal offset are shown in Eqs. (1*n*) and (1*o*)

$$O^g_{i,i+1} = t_{i,i+1} + (\tau_i - \tau_{i+1}) - \Delta^f_{i,i+1} \tag{1n}$$

$$\bar{O}^g_{i+1,1} = \bar{t}_{i+1,i} + (\bar{\tau}_{i+1} - \bar{\tau}_i) - \Delta^f_{i+1,i}$$

$$i = 1,2,\ldots,n-1 \tag{1o}$$

Simulation and Analyses

In this section, we validate the performances of the proposed model. Measures of Effectiveness (MOE_s) acquired by TSIS-CORSIM 6 (2001), including network-wide average delay (sec/veh), average travel speed (km/h), and stop (%), are used to evaluate the performances at each coordinated traffic system. Through the simulations, if the MOE of stop is reduced, the objective of the proposed model can be established. The other two MOE_s are used to evaluate the overall network performances after applying the proposed model. On the basis of objective fairness, this study adopts *Synchro 6.0 user's manual (2004)* as an input interface and then uses traffic simulation software, TSIS-CORSIM 6, to obtain the MOE_s.

Basic Network

In order to analyze the performance of the proposed model, a network consisting of four intersections is created. The four intersections are controlled as a coordinated system. All intersections consist of four lanes on major streets and two lanes on minor streets. The basic conditions for this study include: (1) 3.5 m wide lanes; (2) 5 m wide shoulders; (3) level terrain; and (4) saturation flow rate of 1800 VPH/hg/ln. Fig. 5 and Table 2 illustrate the basic network of this study.

In order to provide sufficient time to pedestrians to cross the street, the minimum green time constraint is added to the model. The minimum green time is calculated using Eq. (2) (National Research Council 1997)

$$G_P = 7.0 + (W/4.0)\text{-}Y \tag{2}$$

Where G_P=minimum green time (sec); W=lane width (ft); and Y=changing interval (sec).

To understand the network performance under different traffic demands, it is assumed that the combined degrees of saturation (DOS) are 70%, 80%, and 90%. The MOE_s of network-wide average delay (sec/veh), average travel speed (km/h) and stop (%) are acquired by using TSIS-CORSIM 6 for the three assumed DOS. However, for the average speed, we only consider major-street approaches for the arterial system.

Comparison of Proposed Model to Synchro

In this section, a formulation proposed by Webster and Cobbe (1966) is used to run five selected cases and to obtain the optimal green splits. By applying the proposed model, the optimal signal cycles and offsets are obtained. The optimal signal cycles in this study are obtained by entering all related proposed equations into the Lingo programming system. The optimal signal cycles, in the Lingo programming system, are designed to fall into a predefined and reasonable cycle range of 60 s to 180 s. Even though Synchro

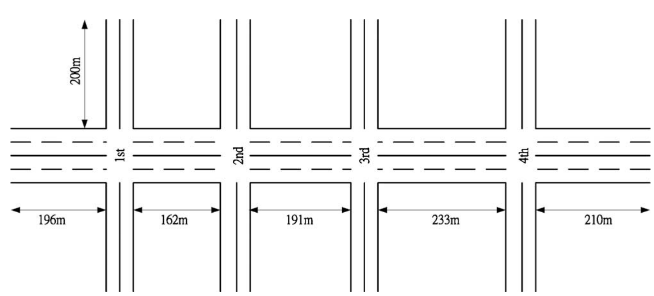

Fig. 5. Geometry and traffic flow of the network

J. Transp. Eng. 2010.136:727-735.

Table 2. Network Traffic Data

Degree of saturation (%)		Approach	First intersection LT	TH	RT	Second intersection LT	TH	RT	Third intersection LT	TH	RT	Fourth intersection LT	TH	RT
70	Major: 50% Minor: 20%	N	52	1,696	50	58	1,708	38	30	1,718	50	32	1,736	32
		S	52	1,700	50	38	1,680	82	50	1,672	78	38	1,716	60
		W	50	250	60	70	240	50	50	246	56	60	252	38
		E	50	260	50	40	270	50	30	258	72	24	272	64
	Major: 40% Minor: 30%	N	52	1,336	50	58	1,348	38	30	1,358	50	32	1,376	32
		S	52	1,340	48	38	1,320	82	50	1,312	78	38	1,336	60
		W	50	420	60	70	420	50	50	430	56	60	442	38
		E	50	440	50	40	450	50	30	438	72	24	452	64
80	Major: 50% Minor: 30%	N	52	1,696	50	58	1,708	38	30	1,718	50	32	1,736	32
		S	52	1,700	48	38	1,680	82	50	1,672	78	38	1,696	60
		W	50	420	60	70	420	50	50	430	56	60	442	38
		E	50	440	50	40	450	50	30	438	72	24	452	64
	Major: 40% Minor: 40%	N	104	1,232	100	116	1,256	76	60	1,276	100	64	1,312	64
		S	104	1,240	96	76	1,200	164	100	1,184	156	76	1,232	120
		W	100	500	120	140	480	100	100	492	112	120	504	76
		E	100	520	100	80	540	100	60	516	144	48	544	128
90	Major: 50% Minor: 40%	N	104	1,592	100	116	1,616	76	60	1,636	100	64	1,672	64
		S	104	1,600	96	76	1,560	164	100	1,544	156	76	1,592	120
		W	100	500	120	140	480	100	100	492	112	120	504	76
		E	100	520	100	80	540	100	60	516	144	48	544	128

also produces optimal signal cycles, the optimal cycle length generated by Synchro decreases as the traffic demand increases (or DOS). According to the findings of Husch and Albeck (2006), Synchro starts with a short cycle length and then optimizes splits. If the split of each phase is not able to clear the critical traffic percentile, Synchro continues increasing cycle length until the critical percentile traffic is cleared.

Once the optimal signal cycles are obtained, the optimal offsets at intersections are acquired by the proposed model. Next, two groups of optimal signal parameters are inputted into CORSIM. In Group 1, the signal cycles and offsets are generated by the proposed model and the splits are generated by Webster's formulation. In Group 2, all three signal timing parameters are generated by Synchro. As for each group and each case, multiple replications (approx. Ten times per group per case) with different random seeds are conducted to acquire performance measures. As for each case, the generated results of each performance measure are then averaged to obtain the mean value. Last, we compare the MOE_s of two groups to validate whether the proposed model can be an alternative option for determining the essential parameters of traffic signal control. The experimental results are presented in Fig. 6.

In Fig. 6, in terms of stop (%), the variations are significant. The proposed model yields lower stops in all five selected cases.

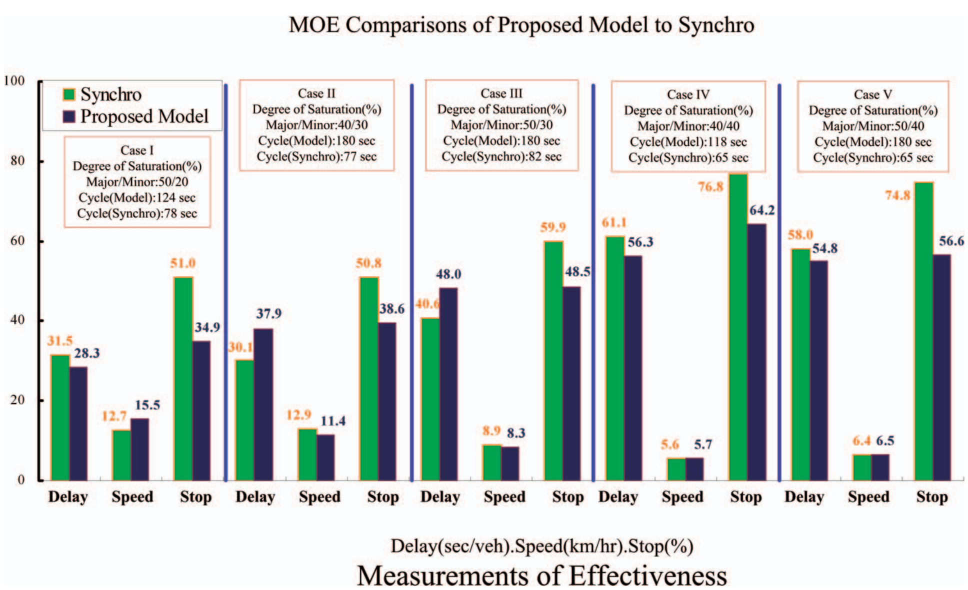

Fig. 6. (Color) MOE comparisons between Synchro and the proposed method

J. Transp. Eng. 2010.136:727-735.

It also yields higher average travel speeds for most of the cases, as well as equivalent or better network-wide average delays than Synchro. This phenomenon is more noticeable as the DOS reaches higher DOS (i.e., 80% DOS in Case IV and 90% DOS in Case V). As the DOS increases, the proposed model produces longer cycle lengths as compared with the values produced by Synchro. The reason for this phenomenon is that the objective function of the proposed model is designed to maximize progression bandwidths. Therefore, the delay-related constraints are not included in the model. No delay-related constraints result in high cycle lengths as the traffic demand increases. However, as the cycle length increases, the time lost between signal phase changes decreases. Therefore, the green time per cycle can be effectively used, and the roadway capacity increased. In contrast, when the traffic demands (or DOS) increase, the optimal cycle lengths generated by Synchro decrease. Consequently, the average delays generated by the proposed model can yield lower values due to sufficient cycle lengths to accommodate high traffic demands. The comparisons in network-wide average delays prove that the proposed model can design adequate signal cycles to satisfy the actual traffic demands. Therefore, the proposed model can be applied as an alternative method in traffic signal planning.

From the MOE_s of network-wide average delay, average travel speed and stop, the optimal green splits are acquired from Webster's formulation and the optimal signal cycles and offsets are calculated by the proposed model. From the CORSIM simulation results, this study found that the proposed model can yield significantly lower stops than Synchro. However, the proposed model yields similar results to those of Synchro in terms of average travel speeds. As for the network-wide average delays, the overall delay difference is insignificant. Under high DOS, the proposed model can yield significantly better delays than Synchro. This phenomenon is attributed to the different optimal signal cycle concept of Synchro. For the proposed model, as the demand increases, signal cycle adjusts to meet and satisfy actual traffic demands. Hence, the proposed model improves the delays generated by Synchro especially under high DOS. The delay improvements can be found in Cases IV and V. As the model is calculated continuously, its suitability for a major street is emphasized.

Summary and Conclusions

Increasing signal timing on an arterial may lead to increasingly difficult-to-achieve progression bands. In order to overcome this dilemma, a MINLP model is applied to develop an optimal arterial-based progression algorithm. This study also introduces the maximum number of intersections that vehicles can traverse through in a signal progression band, the principle of the arrival sequences and the variations in the leading and trailing of adjacent bands to the model, and seek to resolve different traffic situations for arterial intersections. By modifying the objective function, constraints, and calculations of Tsay and Lin's model, the revised model overcomes the shortcomings of Tsay and Lin's model in providing sufficient progression bandwidths for traffic contiguously traveling inbound to (or outbound from) the arterial. The proposed model can accommodate different traffic demands (from low to high DOS) allowing for more flexibility.

As traffic demands increase, the cycle length obtained by Synchro decreases. In order to obtain optimal signal timing, application of the proposed model with the Lingo programming system acquired the optimal signal cycles. MOE_s from CORSIM tests indicate that the proposed model is more effective than Synchro in terms of average travel speeds and stops. From the delay perspective, the overall network-wide average delay difference is insignificant. However, under high DOS, the proposed method can yield better delays than Synchro. Based on the performances of network-wide average delays, average travel speeds and stops, the signal timing acquired from the proposed model can be used as an alternative signal planning tool. However, further additional testing in different types of networks and with different DOS (i.e., over saturation) and arrival types are needed to confirm these findings.

Acknowledgments

This research is dedicated in remembrance of Hsin-Chuan Ku, coauthor, 26-year-old, whose life was cut short by the tragic events of Typhoon Morakot (as known as 88 Typhoon) in Taiwan in August 2009. His dedication and expertise were an essential part of this research. He will not be forgotten.

Appendix. Overall Proposed Model

$$\text{MAX} \sum_{i=1}^{n} [P_i + \overline{P_i} + b \times \max(Q_i^E, Q_i^W)]$$

$$ST \;\; 1/C_2 \leq Z \leq 1/C_1$$

$$\left.\begin{aligned} \tau_i + b_i + W_i + r_i = 1 \\ \bar{\tau}_i + \bar{b}_i + \bar{W}_i + \bar{r}_i = 1 \end{aligned}\right\} \quad i = 1, \ldots, n$$

$$b_i = \Delta_{i-1,i}^f + b_{i-1} + \Delta_{i-1,i}^e \quad i = 2, \ldots, n$$

$$\bar{b}_i = \Delta_{i+1,i}^f + b_i + \Delta_{i+1,i}^e \quad i = 1, \ldots, n-1$$

$$\left.\begin{aligned} -g_i + \tau_i \leq \Delta_{i-1,i}^f \leq g_i - \tau_i \\ -g_i + \tau_i \leq \Delta_{i-1,i}^e \leq g_i - \tau_i \end{aligned}\right\} \quad i = 2, \ldots, n$$

$$\left.\begin{aligned} -\bar{g}_i + \bar{\tau}_i \leq \Delta_{i+1,i}^f \leq \bar{g}_i - \bar{\tau}_i \\ -\bar{g}_i + \bar{\tau}_i \leq \Delta_{i+1,i}^e \leq \bar{g}_i - \bar{\tau}_i \end{aligned}\right\} \quad i = 1, \ldots, n-1$$

$$t_{(i,i+1)} + \bar{t}_{(i+1,i)} + \frac{1}{2}(r_i + \bar{r}_i) - \frac{1}{2}(r_{i+1} + \bar{r}_{i+1}) + (\tau_i - \tau_{i+1})$$

$$-(\Delta_{i,i+1}^f - \Delta_{i-1,i}^e) + (\bar{w}_i - \bar{w}_{i+1}) + \Delta_i - \Delta_{i+1} = I_i \quad i = 1, \ldots, n-1$$

$$\sum_{i=1}^{n-1} \left[\left(\prod_{j=i}^{n-1} \prod_{k \geq j}^{n-1} P_{jk} \right) \times d_i \right] + e_{n-1} = g_{n-1}$$

$$\left.\begin{aligned} (d_i/f_i)Z \leq t_i \leq (d_i/m_i)Z \\ (\bar{d}_i/\bar{f}_i)Z \leq \bar{t}_i \leq (\bar{d}_i/\bar{m}_i)Z \end{aligned}\right\} \quad i = 1, \ldots, n-1$$

$$\left.\begin{aligned} (d_i/h_i)Z \leq (d_i/d_{i+1})t_{i+1} - t_i \leq (d_i/n_i)Z \\ (\bar{d}_{i+1}/\bar{h}_{i+1})Z \leq (\bar{d}_{i+1}/\bar{d}_i)\bar{t}_i - \bar{t}_{i+1} \leq (\bar{d}_{i+1}/\bar{n}_{i+1})Z \end{aligned}\right\} \quad i = 1, \ldots, n-2$$

$$\left.\begin{aligned} \tau_i \times (1/Z) \times S_a \times 6 \leq D_{i-1,i} \\ g_i \times (1/Z) \times \lambda_a \times 6 \leq D_{i,i}^W \end{aligned}\right\} \quad i = 1, \ldots, n$$

J. Transp. Eng. 2010.136:727-735.

$$\left.\begin{aligned}\bar{\tau}_i \times (1/Z) \times S_a \times 6 \le D_{i+1,i}\\ \bar{g}_i \times (1/Z) \times \lambda_a \times 6 \le D^E_{i,i}\end{aligned}\right\} \quad i = 1, \ldots, n$$

$$r_i - \Delta_i \ge \mathrm{MING}_i \quad i = 1, \ldots, n$$

$$\left.\begin{aligned}O^g_{i,i+1} = t_{(i,i+1)} + (\tau_i - \tau_{i+1}) - \Delta^f_{i,i+1}\\ \bar{O}^g_{i+1,1} = \bar{t}_{(i+1,i)} + (\bar{\tau}_{i+1} - \bar{\tau}_i) - \Delta^f_{i+1,i}\end{aligned}\right\} \quad i = 1, \ldots, n-1$$

$$\tau_i, b_i, b, W_i, \Delta^f_{i,i+1}, \Delta^e_{i,i+1}, t_i, \bar{t}_i, O^g_{i,i+1}, \bar{O}^g_{i+1,1} \ge 0$$

$$I_i, P_i, \overline{P_i} \ \text{ are integers}$$

References

Gartner, N. H., Assmann, S. F., Lasaga, F., and Hou, D. L. (1991). "A multi-band approach to arterial traffic signal optimization." *Transp. Res., Part B: Methodol.*, 25(1), 55–74.

Gartner, N. H., and Stamatiadis, C. (2002). "Arterial-based control of traffic flow in urban grid networks." *Math. Comput. Model. Dyn. Syst.*, 35(5–6), 657–671.

Gartner, N. H., and Stamatiadis, C. (2004). "Progression optimization featuring arterial- and route-based priority signal networks." *J. Intell. Transp. Syst.*, 8, 77–86.

Husch, D., and Albeck, J. (2006). *Synchro studio 7*, Trafficware, Sugarland, Tex.

Little, J. D. C. (1966). "The synchronization of traffic signals by mixed-integer linear programming." *Oper. Res.*, 14, 568–594.

National Research Council. (1997). *Highway capacity manual*, TRB, Washington, D.C.

Pillai, R. S., Rathi, A. K., and Cohenb, S. L. (1998). "A restricted branch-and-bound approach for generating maximum bandwidth signal timing plans for traffic networks." *Transp. Res., Part B: Methodol.*, 32, 517–529.

Roess, R. P., Prassas, E. S., and Mcshane, W. R. (2004). *Traffic engineering*, 3rd Ed., Prentice Hall, Englewood Cliffs, N.J.

Stamatiadis, C., and Gartner, N. H., (1996). "Multiband: A program for variable-bandwidth progression optimization of multiarterial traffic networks." *Transp. Res. Rec.*, 1554, 9–17.

Synchro 6.0 user's manual. (2004). Trafficware, Albany, Calif.

Tian, Z., Mangal, V., and Liu, H. (2008). "Effectiveness of lead-lag phasing on progression bandwidth." *Transp. Res. Rec.*, 2080, 22–27.

Tian, Z., and Urbanik, T. (2007). "System partition technique to improve signal coordination and traffic progression." *J. Transp. Eng.*, 133(2), 119–128.

Tsay, H.-S., and Lin, L.-T. (1988). "A new algorithm for solving the maximum progression bandwidth." *Transp. Res. Rec.*, 1194, 15–30.

Webster, F. V., and Cobbe, B. M. (1966). *Traffic signal-Road Research Technical Paper No. 56*, HMSO, London.

Yang, X. K. (2001). "Comparison among computer packages in providing timing plans for Iowa Arterial in Lawrence." *J. Transp. Eng.*, 127(4), 311–318.

J. Transp. Eng. 2010.136:727-735.